JVSTB
JOURNAL OF VACUUM SCIENCE AND TECHNOLOGY B

Method of control of nitrogen content in ZnO films: Structural and photoluminescence properties

J. G. Ma, Y. C. Liu, R. Mu, J. Y. Zhang, Y. M. Lu et al.

Citation: J. Vac. Sci. Technol. B **22**, 94 (2004); doi: 10.1116/1.1641057
View online: http://dx.doi.org/10.1116/1.1641057
View Table of Contents: http://avspublications.org/resource/1/JVTBD9/v22/i1
Published by the AVS: Science & Technology of Materials, Interfaces, and Processing

Related Articles

Substrate-biasing during plasma-assisted atomic layer deposition to tailor metal-oxide thin film growth
J. Vac. Sci. Technol. A 31, 01A106 (2013)

Substrate temperature and electron fluence effects on metallic films created by electron beam induced deposition
J. Vac. Sci. Technol. B 30, 051805 (2012)

Effect of O2 gas partial pressure on mechanical properties of Al2O3 films deposited by inductively coupled plasma-assisted radio frequency magnetron sputtering
J. Vac. Sci. Technol. A 30, 051511 (2012)

Tetragonal or monoclinic ZrO2 thin films from Zr-based glassy templates
J. Vac. Sci. Technol. A 30, 051510 (2012)

Phase identification and control of thin films deposited by co-evaporation of elemental Cu, Zn, Sn, and Se
J. Vac. Sci. Technol. A 30, 051201 (2012)

Additional information on J. Vac. Sci. Technol. B

Journal Homepage: http://avspublications.org/jvstb
Journal Information: http://avspublications.org/jvstb/about/about_the_journal
Top downloads: http://avspublications.org/jvstb/top_20_most_downloaded
Information for Authors: http://avspublications.org/jvstb/authors/information_for_contributors

ADVERTISEMENT

Method of control of nitrogen content in ZnO films: Structural and photoluminescence properties

J. G. Ma and Y. C. Liu[a)]
Key Laboratory of Excited State Processes, Changchun Institute of Optics, Fine Mechanics, and Physics, Chinese Academy of Science, Changchun 130033, People's Republic of China

R. Mu
Center for Photonic Materials and Devices, Fisk University and Department of Physics and Astronomy, Vanderbilt University, Nashville, Tennessee 37208

J. Y. Zhang, Y. M. Lu, D. Z. Shen, and X. W. Fan
Key Laboratory of Excited State Processes, Changchun Institute of Optics, Fine Mechanics, and Physics, Chinese Academy of Science, Changchun 130033, People's Republic of China

(Received 10 July 2003; accepted 10 November 2003; published 14 January 2004)

In this article, nitrogen doped ZnO thin films with various nitrogen concentrations were obtained by thermal processing of zinc oxynitride alloy films prepared by radio frequency reactive magnetron sputtering. X-ray photoelectron spectroscopy study shows that varying the annealing temperature can modulate the concentration of nitrogen in ZnO. X-ray diffraction and Raman scattering measurements were employed to investigate the structural changes of ZnO films induced by the introduction of nitrogen. The results of the temperature-dependent photoluminescence measurements suggest that the optical properties of ZnO thin films are strongly influenced by nitrogen incorporation. With this technique, the binding energy of the nitrogen acceptor is also estimated. [DOI: 10.1116/1.1641057]

I. INTRODUCTION

Zinc oxide (ZnO) is a II–VI compound semiconductor with a wide direct band gap of 3.37 eV at room temperature.[1] It has an exciton binding energy of 60 meV larger than that of GaN and high exciton emission efficiency. Because of these features, ZnO has become a promising candidate for applications in blue and ultraviolet (UV) light sources and as a UV detector. Although several groups have recently reported room-temperature optically pumped lasing of ZnO in the blue and UV range,[2–4] to obtain a consistent, reliable, and high-quality *p*-type ZnO semiconducting material is the bottleneck for the practical applications of ZnO. The reason is that many intrinsic donorlike defects, such as oxygen vacancy (V_O), zinc interstitials (Zn_i), and zinc antisite defects (Zn_O), are formed during the film growth process. However, there have been a few reports about the fabrication of *p*-type ZnO recently by using As or N as individual dopants,[5,6] and both Ga and N as a codopant.[7] Moreover, based on the theoretical calculations,[8] nitrogen may be a better candidate of dopants for *p*-type ZnO fabrication.

Radio-frequency (rf) reactive magnetron sputtering is a flexible technique for the deposition of various films at low temperature. However, it is difficult to achieve an effective and sufficient doping of N in ZnO films with N_2 and O_2 mixtures as reactive gas. The possible reason is that the oxidizing power of oxygen is much stronger than that of nitrogen. Thus, a technique is presented in this article. Zinc oxynitride (ZnON) alloy films are fabricated with rf reactive magnetron sputtering. Then, a controlled thermal process is used to achieve nitrogen-doped ZnO films.

II. EXPERIMENT

ZnON films were deposited on crystalline silicon (100) substrates by rf reactive magnetron sputtering. The sputtering chamber was evacuated to a base pressure below 3×10^{-4} Pa with a turbomolecular pump. A metallic zinc disk with a purity of 99.999% (5N) was used as the sputtering target. Before deposition, the target was etched with diluted nitric acid to remove the contamination. The target–substrate distance was maintained at 60 mm. The substrate temperature was controlled at 200 °C. The working pressure in the chamber was kept at 1.0 Pa during the film growth. The rf power was kept at 100 W. Ultrapure (5N) Ar, N_2, and O_2 gas mixtures were introduced into the sputtering chamber through a set of mass flow controllers with the flow rates of 200 sccm, 20 sccm, and 80 sccm, respectively. These are optimized flow rates for growing the ZnON films.

After deposition, the samples were cleaved into smaller pieces and transferred into a standard diffusion furnace where thermal annealing was carried out. A typical thermal annealing time was 1 h at a chosen temperature under a pure oxygen environment with the oxygen flow rate of 1 liter per minute. X-ray diffraction (XRD) spectra were collected with a D/max-RA x-ray spectrometer (Rigaku International Corp., Japan) with Cu $K\alpha$ radiation of 0.1543 nm to obtain the structural information of the films. Chemical bonding states and compositions of the films were examined by x-ray photoelectron spectroscopy (XPS) at room temperature with a VG ESCALAB MK II x-ray photoemission spectrometer (VG Scientific, East Grinstead, UK). Low-temperature and

[a)]Author to whom correspondence should be addressed at: Center for Advanced Optoelectronic Functional Material Research, Northeast Normal People's Republic of China; electronic mail: ycliu@nenu.edu.cn

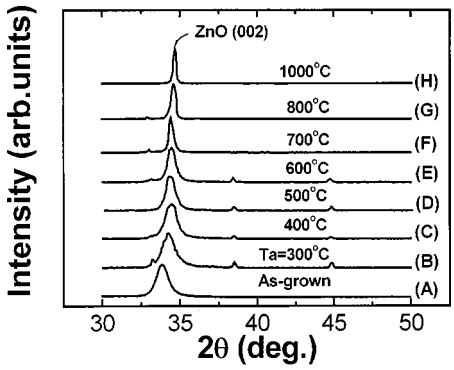

FIG. 1. XRD spectra of the samples that were annealed at different temperatures: (A) as-grown, (B) 300 °C, (C) 400 °C, (D) 500 °C, (E) 600 °C, (F) 700 °C, (G) 800 °C, and (H) 1000 °C.

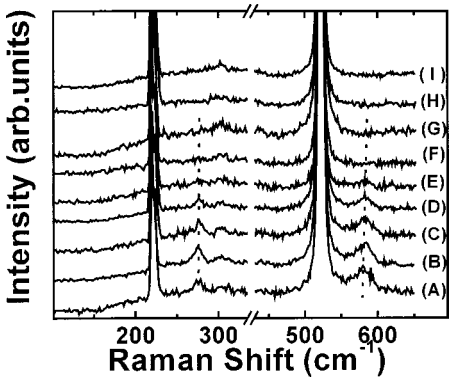

FIG. 2. Raman spectra of the samples annealed at different temperatures: (A) as-grown, (B) 300 °C, (C) 400 °C, (D) 500 °C, (E) 600 °C, (F) 700 °C, (G) 800 °C, (H) 900 °C, and (I) 1000 °C.

temperature-dependent photoluminescence (PL) spectra were also measured to study the influence of N doping on the luminescence properties of ZnO films. The 325 nm line of a He–Cd laser was employed as the excitation light. To investigate the local vibration modes affected by nitrogen incorporating into ZnO films, Raman scattering spectra were obtained using the 488 nm line of an argon-ion laser. Both PL and Raman spectra were collected with a microprobe system made by Jobin–Yvon Company in France.

III. RESULTS AND DISCUSSION

The structure of N-doped ZnO thin films was analyzed by XRD measurement as shown in Fig. 1. Figures 1(A)–1(H) correspond to the XRD spectra of the as-grown and annealed samples at 300, 400, 500, 600, 700, 800, and 1000 °C, respectively. For sample A, the XRD spectrum shows a broad diffraction peak at 33.64°, which located between the (002) peak of ZnO (34.42°) and the (222) peak of Zn_3N_2 (31.66°), suggesting the formation of ZnON alloy. When the sample was annealed at 300 °C in an oxygen ambient for 1 h, shown in Fig. 1(B), the diffraction peak moves to 34.14°, which is close to the diffraction peak of the (002) of ZnO. Hence, it is suggestive that the ZnON alloy film starts to transform to ZnO film. With the increase of annealing temperature, the diffraction peak further shifts to larger angle side. At the annealing temperature of 1000 °C, a strong and sharp peak at 34.41° is observed, which coincide with ZnO (002) diffraction. The calculated *d*-spacing value decreases from 0.266 to 0.260 nm with the increase of annealing temperature as shown in Table I. This agrees well with the Futsuhara's results.[9] A possible reason for the shift of the diffraction peak is that N atom has a larger atomic radius than O atom. Thus, the bond length of N–Zn is expected to be larger than that of O–Zn.

Another observation is that the full width at half maximum (FWHM) of this diffraction peak, summarized in Table I, (1) increased from 0.801° for the as-grown sample to 0.831° when annealed at 300 °C and (2) decreased from 0.801° to 0.191° when annealed above 300 °C up to 1000 °C. The possible explanation of the broad diffraction peak for the as-grown sample may originate from the poor crystalline quality of the film. In the current experiment, both rf power and the substrate temperature are kept at low values (100 W and 200 °C) to avoid melting the Zn target. Because of the lower substrate temperature and the lower kinetic energy of the Zn atoms and N ions, deposited materials are unable to diffuse on the substrate surface to form a high-quality film. In addition, the deactivated N ions can also be trapped in the film taking the interstitial sites. The increase in the FWHM for the sample annealed at 300 °C with respect to the as-grown sample may be due to an increase in crystalline disorder partly from the further Zn—N bond formation, diffusion of the interstitial nitrogen, and certain level of oxidation in the film. At the same time, the temperature is too low to induce any recrystallization and growth process. Similarly, that the linewidth narrows with the increase of annealing temperature is the result of recrystallization and growth processes in the film when the sample is further oxidized.

Figure 2 shows the Raman spectra of the as-grown ZnON and thermally annealed films at different temperatures. According to the selection rules, both E_2 and A_1 [longitudinal optical (LO)] modes are expected in Raman spectra when the experiments are taken in a backscattering geometry. Two E_2

TABLE I. Variation of *d* spacing and FWHM of ZnO (002) diffraction peak with the increase of the annealing temperature.

T (°C)	As-grown	300	400	500	600	700	800	1000
d (nm)	0.2664	0.2631	0.2629	0.2624	0.2619	0.2622	0.2609	0.2603
FWHM	0.801	0.831	0.729	0.596	0.523	0.312	0.302	0.191

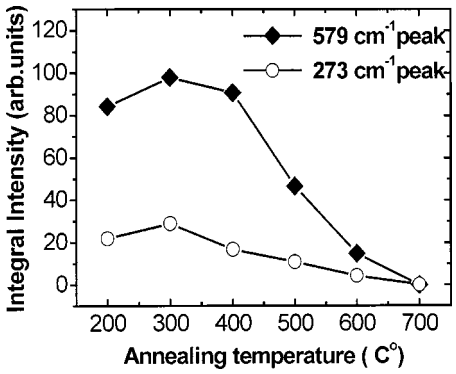

FIG. 3. Variation of the integral intensities of Raman peaks at 273 cm^{-1} (○) and 579 cm^{-1} (◆) with the annealing temperature.

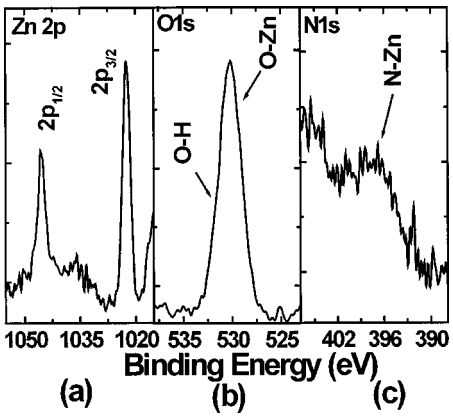

FIG. 4. Zn 2*p* (a), O 1*s* (b), and N 1*s* (c) spectra of the sample annealed at 600 °C.

modes are observed at 101 cm^{-1} and 437 cm^{-1}. One A_1 (LO) mode is located at 574 cm^{-1}. In addition, two peaks can also be observed at 273 cm^{-1} and 579 cm^{-1}, as illustrated in Fig. 2. These two bands do not belong to the Raman spectra of ZnO. According to the results reported by Kaschner *et al.*,[10] these peaks can be interpreted in terms of nitrogen-related local vibration modes. Figure 3 illustrates the change of the integral intensities of these two peaks as a function of annealing temperature. Although the absolute intensity is not same for these two peaks, the trend of the integral intensity of the two peaks follows the same pattern. Further, these two peaks reach their maximum values when the sample was annealed at 300 °C. Then, the intensities of the peaks decrease monotonically with increasing annealing temperature from 300 °C to 700 °C. No further increase is observed when the temperature is above 700 °C. It should be pointed out that this trend in the integral intensity is also reflected in the linewidth change of the (002) ZnO peak in XRD spectra, as summarized in Table I. As discussed before, when the sample is annealed at 300 °C, the further Zn—N bond formation, oxidation, and the diffusion of nitrogen may be the dominant processes. Little recrystallization and growth take place. Hence, the increase of the integral intensities of the Raman peaks at 273 cm^{-1} and 579 cm^{-1} is the reflection of an increase of (1) Zn–N formation and (2) the crystalline disorder of the film. As the temperature is increased from 400 °C to 1000 °C in oxygen ambient, oxidation reaction, and film recrystallization and growth become the dominant processes. As a result, the Zn—N bonds are gradually replaced by Zn—O bonds, which leads to the decrease of the band intensities of at 273 cm^{-1} and 579 cm^{-1}. These two Raman peaks disappear when the annealing temperature reaches 700 °C and above.

Figure 4 shows the typical XPS spectra of the sample annealed at 600 °C. The core levels of Zn 2*p*, N 1*s*, and O 1*s* peaks were observed. The binding energy of the Zn $2p_{3/2}$ peak is located at 1022.8 eV, as illustrated in Fig. 4(a). The O 1*s* peak is split into two peaks, as shown in Fig. 4(b). The peak at 530.8 eV can be attributed to Zn—O bond formation while the peak at 532.3 eV can be attributed to the O—H bond formation. The formation of O—H bonds might have resulted from the hydrolysis of the film surface when it is exposed to air. Figure 4(c) shows N 1*s* spectrum in which N 1*s* peak is located at 396.2 eV. The N 1*s* peak shows a chemical shift in comparison with the N 1*s* peak for free amine (near 398.8 eV), which indicates the formation of Zn—N bonds. Gaussian curve fitting was employed to fit the peak associated with O 1*s* and N 1*s* bonds of the XPS spectra for the samples annealed at various temperatures. The fitted data were plotted in Fig. 5. The results show that the integral intensity of O 1*s* peaks due to Zn—O bonds increases with the increase of the annealing temperature. The integral intensity of N 1*s* peaks due to Zn—N bonds, however, decreases monotonically with the increase of the annealing temperature up to 800 °C. When the sample was annealed above 800 °C, N 1*s* intensity is beyond the instrumental limits.

To study the influence of nitrogen doping on the optical properties of ZnO, the low-temperature emission spectra of the samples annealed at 600 °C and 1000 °C were measured. Figures 6(a) and 6(b) show the low-temperature PL spectra of the samples annealed at 600 °C and 1000 °C, respectively. It is known that the sample annealed at 600 °C is N-doped

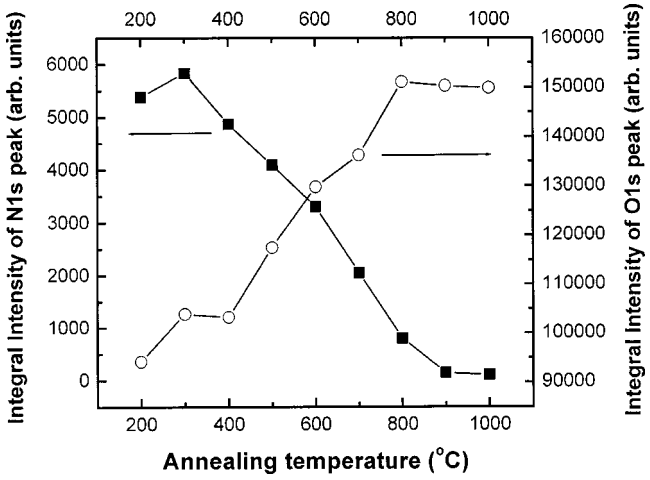

FIG. 5. Variation of the integral intensities of N 1*s* and O 1*s* peaks in XPS spectra with the increase of the annealing temperature.

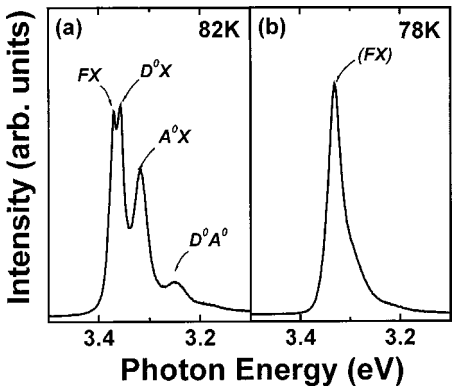

FIG. 6. PL spectra of the sample anncaled at 600 °C (a) and the sample annealed at 1000 °C (b), which were measured at 82 K and 78 K, respectively.

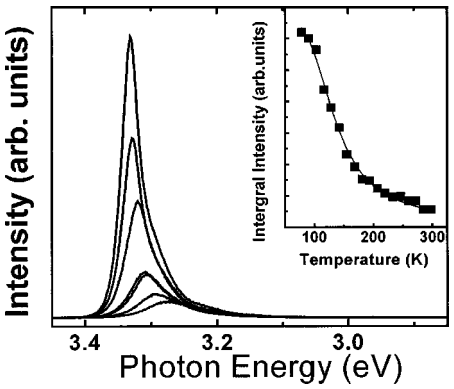

FIG. 7. Temperature-dependent PL spectra of the sample that annealed at 1000 °C with the temperature varying from 78 K to 298 K. The inset shows the plot of the integral PL intensities against temperature for the sample annealed at 1000 °C. Solid symbols are experimental data and solid line is fit using the equation: $I(T)=I_0/[1+C^* \exp(-E/KT)]$.

ZnO film, while the sample annealed at 1000 °C is pure ZnO. In Fig. 6(a), there are a series of sharp bands. Among them, the strongest one is at 3.358 eV. Some weaker bands follow it at 3.371, 3.317, and 3.251 eV. According to the band position, the PL at 3.358 eV can be assigned to the emission of donor-bound excitons (D^0X), while the peak at 3.371 eV is assigned to the emission of free excitons (FX). These values agree well with the reported values for D^0X and FX.[11–13] However, it is difficult to identify the origin of two peaks at 3.317 and 3.251 eV. They do not belong to the I_6 to I_{11} lines of ZnO as reported previously[14] and cannot be attributed to LO-phonon replicas of D^0X or FX either. The reason is that the energy separation between two peaks and D^0X and FX cannot match to integer multiples of the LO-phonon energy (72 meV) of ZnO. Look *et al.*[15] reported recently that there is a strong line at 3.317 eV in low-temperature PL spectra of N-doped ZnO. They have attributed the emission to an acceptor-bound exciton (A^0X) associated with the substitutional nitrogen in the ZnO lattice. As discussed above, the sample annealed at 600 °C is N-doped ZnO film. Thus, it is natural to consider that the band at 3.317 eV originated from A^0X related to substitutional nitrogen. The band at 3.251 eV is from the donor–acceptor pair (D^0A^0) transitions.

In general, it is possible to estimate the acceptor binding energy E_A by using the equation

$$E_A=E_G-E_D-E(D^0A^0)+e^2/4\pi\epsilon r,$$

where E_G, E_D, and $E(D^0A^0)$ are the bandgap of the material, donor energy, and the energy of donor–acceptor pair, respectively. ϵ is the dielectric constant, and r is the pair separation. For ZnO, the band gap is 3.43 eV at 82 K and the donor energy is known to be 60 meV.[13] The calculated E_A from the equation above is 120 meV, which is comparable to the value reported by others.[6,15] In comparison, the binding energies of the nitrogen acceptors in ZnSe and ZnS are 110 meV (Refs. 16 and 17) and 190 meV,[18] respectively, so the binding energy of the acceptor in ZnO of 120 meV is acceptable. In contrast to Fig. 6(a), Fig. 6(b) has only one sharp peak at 3.330 eV with a small shoulder at the low-energy side. This PL spectrum is typical for pure ZnO emission suggesting that the 1000 °C anneal eliminated all the N dopant and replaced it by O.

Figure 7 show the temperature-dependent PL spectra of the sample in Fig. 6(b) in the temperature ranging from 78 K to 297 K. The identification of the peak at 3.330 eV can be performed by the fit to the integral peak intensity below. The temperature-dependent integral intensity of the peak at 3.330 eV is illustrated as an inset of Fig. 7. As a rough estimation, the thermal quenching of luminescence intensity of an exciton can be expressed as

$$I(T)=I_0/[1+C^* \exp(-E/KT)],$$

where C contains the ratios of optical-collection efficiencies and effective degeneracy between unbound and bound states, E is the thermal activation energy, I_0 is a constant, and T is absolute temperature.[19] By fitting the experimental data to the formula above, the value obtained for E is 56 meV, which is comparable with the binding energy of the free exciton of ZnO quoted in literature of 60 meV. According to the results of XRD and XPS measurements, when the annealing temperature reached 1000 °C, ZnO alloy films have completely transformed into ZnO. So it can be concluded that the emission at 3.330 eV originated from the free exciton of pure ZnO. A single peak dominating the PL spectrum, even at 78 K, indicates that ZnO film with good quality is obtained once it is annealed at 1000 °C. By comparing the spectra in Figs. 6(a) and 6(b), we can find that the FX peak undergoes a redshift with the annealing temperature increasing from 600 °C to 1000 °C. Thus, it may be argued that the redshift of the FX peak is due to the increase of ZnO nanocrystal size with the increase of annealing temperature. The peak due to A^0X does not appear in Fig. 6(b). The disappearance of the A^0X peak in Fig. 6(b), then, confirms that the A^0X peak is related to the nitrogen dopant in ZnO.

IV. CONCLUSION

We have fabricated nitrogen-doped ZnO thin films with various nitrogen concentrations by thermal treatment of zinc oxygnitride alloy films prepared by rf reactive magnetron sputtering in an oxygen ambient. XRD measurements demonstrate a transformation process from ZnON alloy to ZnO with an increase of annealing temperature. The Raman spectra of N-doped ZnO films show two spectral features at 273 cm^{-1} and 579 cm^{-1} that can be assigned to N-related vibration modes. XPS results indicate the formation of Zn—N bonds in N-doped ZnO films. All results suggest that N has been doped into ZnO thin films. The optical properties of N-doped ZnO films were characterized by low-temperature PL spectra. The binding energy of the acceptor-bound excitons is estimated at about 120 meV by analyzing the low-temperature PL results of the samples annealed at 600 °C and 1000 °C.

ACKNOWLEDGMENTS

This work is supported by the Program of CAS Hundred Talents, the National Natural Science Foundation of China (60176003), Excellent Young Teacher Foundation of Ministry of Education of China, and the Foundational Excellent Researcher to Go beyond Century of the Ministry of Education of China. The Major Project of the National Natural Science Foundation of China No. 60336020, The ''863'' Advanced Technology Research Program No. 2001AA31112, The Knowledge Innovation Program of CIOMP.

[1]C. Klingshirn, Phys. Status Solidi B **71**, 547 (1975).
[2]D. M. Bagnall, Y. F. Chen, Z. Zhu, T. Yao, M. Y. Shen, and T. Goto, Appl. Phys. Lett. **73**, 1038 (1998).
[3]Z. K. Tang, G. K. L. Wong, P. Yu, M. Kawasaki, A. Ohtomo, H. Koinuma, and Y. Segewa, Appl. Phys. Lett. **72**, 3270 (1998).
[4]X. T. Zhang, Y. C. Liu, L. G. Zhang, J. Y. Zhang, Y. M. Lu, D. Z. Shen, W. Xu, G. Z. Zhong, X. W. Fan, and X. G. Kong, J. Appl. Phys. **92**, 3293 (2002).
[5]Y. R. Ryu, S. Zhu, D. C. Look, J. M. Wrobel, H. M. Jeong, and H. W. White, J. Cryst. Growth **216**, 330 (2000).
[6]K. Minegishi, Y. Koiwai, Y. Kikuchi, and K. Yano, Jpn. J. Appl. Phys., Part 2 **36**, L1453 (1997).
[7]M. Joseph, H. Tabata, and T. Kawai, Jpn. J. Appl. Phys., Part 2 **38**, L1205 (1999).
[8]Y. Yan and S. B. Zhang, Phys. Rev. Lett. **86**, 5723 (2001).
[9]M. Futsuhara, K. Yoshioka, and O. Takai, Thin Solid Films **317**, 322 (1998).
[10]A. Kaschner, U. Haboeck, and M. Strassburg, Appl. Phys. Lett. **80**, 1909 (2002).
[11]X. Q. Wang, S. R. Yang, X. T. Yang, D. Liu, and Y. T. Zhang, J. Cryst. Growth **243**, 12 (2002).
[12]N. Ohashi, T. Sekiguchi, and K. Aoyama, J. Appl. Phys. **91**, 3658 (2002).
[13]D. C. Reynolds, D. C. Look, and B. Jogai, Phys. Rev. B **57**, 12151 (1998).
[14]J. Gutowski, N. Presser, and I. Broser, Phys. Rev. B **38**, 9746 (1988).
[15]D. C. Look, D. C. Reynolds, C. W. Litton, R. L. Jones, D. B. Eason, and G. Cantwell, Appl. Phys. Lett. **81**, 1830 (2002).
[16]W. Stutius, J. Cryst. Growth **59**, 1 (1982).
[17]A. Ohki, N. Shibata, and S. Zebutsu, Jpn. J. Appl. Phys., Part 2 **27**, L909 (1988).
[18]L. Svob, C. Thiandoume, A. Lusson, M. Bouanani, Y. Marfaing, and O. Gorochov, Appl. Phys. Lett. **76**, 1695 (2000).
[19]D. Bimberg, M. Sondergeld, and E. Grobe, Phys. Rev. B **4**, 3451 (1971).